

## The Voronoi diagram of three arbitrary lines in $\mathbb{R}^3$

Hazel Everett, Christian Gillot, Daniel Lazard, Sylvain Lazard, Marc Pouget

► **To cite this version:**

Hazel Everett, Christian Gillot, Daniel Lazard, Sylvain Lazard, Marc Pouget. The Voronoi diagram of three arbitrary lines in  $\mathbb{R}^3$ . 25th European Workshop on Computational Geometry - EuroCG'09, Mar 2009, Bruxelles, Belgium. pp.297-300, 2009. <inria-00425378>

**HAL Id: inria-00425378**

**<https://hal.inria.fr/inria-00425378>**

Submitted on 21 Oct 2009

**HAL** is a multi-disciplinary open access archive for the deposit and dissemination of scientific research documents, whether they are published or not. The documents may come from teaching and research institutions in France or abroad, or from public or private research centers.

L'archive ouverte pluridisciplinaire **HAL**, est destinée au dépôt et à la diffusion de documents scientifiques de niveau recherche, publiés ou non, émanant des établissements d'enseignement et de recherche français ou étrangers, des laboratoires publics ou privés.

# The Voronoi diagram of three arbitrary lines in $\mathbb{R}^3$

Hazel Everett<sup>†</sup>   Christian Gillot<sup>†</sup>   Daniel Lazard<sup>‡</sup>   Sylvain Lazard<sup>†</sup>   Marc Pouget<sup>†</sup>

## Abstract

In this paper we study the Voronoi diagram of lines in  $\mathbb{R}^3$ . The Voronoi diagram of three lines in general position was studied in [8]. In this paper we complete this work by presenting a complete characterization of the Voronoi diagram of three arbitrary lines in  $\mathbb{R}^3$ . As in the general case, we prove that the arcs of trisectors are always monotonic in some direction and we show how to separate the connected components and to sort points along each arc of a trisector using only rational linear semi-algebraic tests. These results are important for the robust computation of the Voronoi diagram of polyhedra.

## 1 Introduction

Voronoi diagrams are ubiquitous objects of computational geometry. The most familiar and intuitive example is the Voronoi diagram of points in the plane with the Euclidean metric. Many extensions have been studied with higher dimension spaces, different metrics and/or other sites than points. For point sites in any dimension, the complexity of Voronoi diagrams is well understood. Optimal algorithms for their construction are known and robust efficient implementations are available (see for instance [1]). Still some important problems remain and are addressed in recent papers. For linear objects (segments and polygons) in two dimensions, the theory and implementations are also well studied [10].

In contrast, for lines, segments, and polyhedra in three dimensions much less is known. Even the combinatorial complexity of the Voronoi diagram of  $n$  lines or line segments in  $\mathbb{R}^3$  is not yet settled. The best known lower (resp. upper) bound is  $\Omega(n^2)$  (resp.  $O(n^{3+\epsilon})$ ) [15]. From an algorithmic point of view, most of the previous work focused on computing the medial axis of a polyhedron,

*i.e.*, a subset of the Voronoi diagram of the faces of the polyhedron [4, 12]. There have been many papers reporting algorithms for computing approximations of the Voronoi diagram (see for instance [5, 7]). On the other hand, as far as we know, only one algorithm has been proposed, following the paradigm of exact geometric computing [4]. This algorithm is nevertheless incomplete since it does not handle the case of singular one-dimensional Voronoi cells. Recently, some progress has been made on the related problem of computing arrangements of quadrics (each cell of the Voronoi diagram is a cell of such an arrangement) [2, 13, 14].

In this paper, we study the Voronoi diagram of three lines in  $\mathbb{R}^3$  with the Euclidean metric. This is the first mandatory step on the way to design a robust and effective implementation of Voronoi diagrams of three-dimensional linear objects. We provide here a complete characterization of the Voronoi diagram of three arbitrary lines in  $\mathbb{R}^3$ . This completes the study of three lines, the case of three lines in general position having been studied in [8]. In particular, we identify those configurations having a singular one-dimensional Voronoi cell, information required to overcome the shortcoming of Culver's algorithm for the exact computation of the medial axis of a polyhedron [4].

**Definitions and notations.** The Voronoi diagram of a set of lines  $S$  is a partition of  $\mathbb{R}^3$  into regions called cells associated with subsets  $s$  of  $S$ . The cell  $V(s)$  consists of the set of points equidistant to the lines of  $s$  and strictly closer to those lines than to any other line. The distance between a point  $p$  and a line  $s$ , is defined as the minimum Euclidean distance between the point and any point on the line.

The Voronoi diagram of pairwise skew lines consists of cells of dimension  $k$  determined by  $4 - k$  lines,  $0 \leq k \leq 3$ . When the lines are no longer skew, a cell determined by  $4 - k$  lines may have dimension strictly smaller than  $k$ . For convenience, in the following a cell of dimension  $k$  (or  $k$ D cell) denotes a cell determined by  $4 - k$  lines, even if its dimension is smaller than  $k$ . In addition, we call bisec-

<sup>†</sup>LORIA - INRIA Lorraine - University Nancy 2, [Firstname.Name@loria.fr](mailto:Firstname.Name@loria.fr)

<sup>‡</sup>LIP6 - INRIA Rocquencourt - University Pierre et Marie Curie, [Firstname.Name@lip6.fr](mailto:Firstname.Name@lip6.fr)

tor (resp. trisector) the dimension two (resp. one) cell of the Voronoi diagram of two (resp. three) lines. The cells are not necessarily connected even in the generic case [8] and when the lines intersect, the number of connected components, as we shall see, may increase. One way of handling intersecting objects is to subdivide them into non-intersecting pieces; for example, in the case of line segments in 2D, intersecting segments are partitioned into points and open segments [9]. Following this approach, one could handle intersecting lines by subdividing them into points, open rays and open segments. Since the bisector of two open segments is typically computed by first computing the bisector of their supporting lines, this approach also requires understanding the nature of the cells in the case of intersecting lines.

## 2 Results

Our main results are summarized in the following theorems which describe the cells of dimension one and two of the Voronoi diagram of three lines, see Table 1 for a more precise description.

**Theorem 1** *The trisector of three lines is*

- (i) *a non-singular quartic if the three lines are pairwise skew but not all parallel to a common plane nor on the surface of a hyperboloid of revolution, (see fig. 1)*
- (ii) *a cubic and a line if the three lines are pairwise skew and lie on the surface of a hyperboloid of revolution,*
- (iii) *a nodal quartic if the three lines are pairwise skew and are all parallel to a common plane,*
- (iv) *one or two parabolas or hyperbolas if there is exactly one pair of coplanar lines,*
- (v) *between 0 and 4 lines if there are two pairs of coplanar lines.*

*In all cases, each branch of the trisector is monotonic in some direction.*

**Theorem 2** *A cell of dimension two of a Voronoi diagram of three lines consists of up to four connected components of hyperbolic paraboloids or planes.*

This characterization yields some fundamental properties of the Voronoi diagram of three lines which are likely to be critical for the analysis of the complexity and the development of efficient algorithms for computing Voronoi diagrams and medial axis of lines or polyhedra. In particular, we obtain the following:

**Theorem 3** *There are rational linear semi-algebraic tests for*

- (i) *given a point on a 2D cell, deciding on which of the connected components of the cell it lies,*
- (ii) *given a point on the trisector, deciding on which of the branches of the trisector it lies,*
- (iii) *ordering points on each branch of the trisector, knowing that they lie on the trisector.*

While the proofs primarily use basic notions from geometry and algebra, such as the classification of conics, it also relies on two recent results, the classification of quadric intersections [6], and a characterization of the common tangents to spheres [3].

## 3 Concluding remarks

We've given here a complete characterization of the Voronoi diagram of three lines. The results are necessary for the robust, exact computation of the Voronoi diagram of lines and the medial axis of polyhedra.

## References

- [1] F. Aurenhammer and R. Klein. Voronoi diagrams. In J. R. Sack and J. Urrutia, editors, *Handbook of computational geometry*, chapter 5, pages 201–290. Elsevier Publishing House, December 1999.
- [2] E. Berberich, M. Hemmer, L. Kettner, E. Schömer, and N. Wolpert. An exact, complete and efficient implementation for computing planar maps of quadric intersection curves. In *SoCG'05*, pages 99–115, 2005.
- [3] C. Borcea, X. Goaoc, S. Lazard, and S. Petitjean. Common tangents to spheres in  $\mathbb{R}^3$ . *DCG*, 35(2):287–300, 2006.
- [4] T. Culver. *Computing the Medial Axis of a Polyhedron Reliably and Efficiently*. PhD thesis, University of North Carolina at Chapel Hill, 2000.
- [5] T. K. Dey and W. Zhao. Approximate medial axis as a voronoi subcomplex. In *SMA '02*, pages 356–366, New York, NY, USA, 2002. ACM Press.
- [6] L. Dupont, D. Lazard, S. Lazard, and S. Petitjean. Near-optimal parameterization of the intersection of quadrics: II. A classification of pencils. *Journal of Symbolic Computation*, 2007. In press (24 pages).
- [7] M. Etzion and A. Rappoport. Computing Voronoi skeletons of a 3-d polyhedron

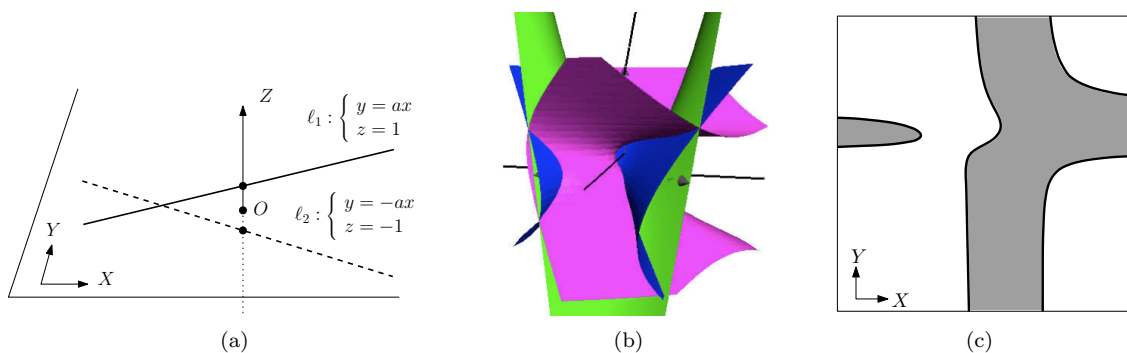


Figure 1: (a) The standard configuration of two skew lines. (b) The trisector of three skew lines, which is the intersection of two hyperbolic paraboloids, is a non-singular quartic. (c) Orthogonal projection of a 2D cell on a plane  $\mathcal{P}$  with coordinate system  $(X, Y)$ ; the plane's normal is parallel to the common perpendicular of  $\ell_1$  and  $\ell_2$  and the  $X$  and  $Y$ -axes are parallel to the two bisector lines (in  $\mathcal{P}$ ) of the projection of  $\ell_1$  and  $\ell_2$  on  $\mathcal{P}$ . The 2D cell is bounded by four branches of the trisector.

Configuration of lines	Trisector	Bisector type			No. CC		
		$\mathcal{H}_{1,2}$	$\mathcal{H}_{1,3}$	$\mathcal{H}_{2,3}$	$V_{1,2}$	$V_{1,3}$	$V_{2,3}$
<b>Three pairwise skew lines</b>							
Fig. 2(a) Not all parallel to a common plane nor on a hyperboloid of revolution	non-singular quartic	HP	HP	HP	2	2	2
Fig. 2(b) On a hyperboloid of revolution	cubic and a line	HP	HP	HP	2	2	2
Fig. 2(c) All parallel to a common plane	nodal quartic	HP	HP	HP	1	1	2
<b>One pair of coplanar lines</b>							
Fig. 2(d) One pair intersecting, third skew, not in a parallel plane	two hyperbolas <sup>s</sup>	HP	HP	2P	3	3	2
Fig. 2(e) One pair intersecting, third in a parallel plane	two parabolas <sup>s</sup>	HP	HP	2P	2	2	1
Fig. 2(f) One pair parallel, third skew, not in a parallel plane	one hyperbola	HP	HP	P	2(1)	1	1(2)*
Fig. 2(g) One pair parallel, third in a parallel plane	one parabola	HP	HP	P	1	1	1
<b>Two pairs of coplanar lines</b>							
Fig. 2(h) Two intersecting pairs	four lines <sup>s</sup>	HP	2P	2P	4	3	3
Fig. 2(i) One pair parallel, one pair intersecting	two lines <sup>s</sup>	HP	2P	P	2	1	2
<b>Three pairs of coplanar lines in three distinct planes</b>							
Fig. 2(j) Three pairwise parallel lines	one line	P	P	P	1	1	1
Fig. 2(k) Three concurrent lines	four lines <sup>s</sup>	2P	2P	2P	4	4	4
<b>Three coplanar lines</b>							
Fig. 2(l) Three parallel lines	empty set	P	P	$\emptyset$	1	1	0
Fig. 2(m) Two parallel lines, the third one intersects them	two lines	P	2P	2P	2	1	1
Fig. 2(n) Three concurrent lines	one line	2P	2P	2P	2	2	2
Fig. 2(o) Three pairwise intersecting lines (not in a point)	four lines	2P	2P	2P	2	2	2

Table 1: Classification of the trisectors and 2D cells of three lines. Whenever there are two skew lines amongst the three lines, we assume they are labeled  $\ell_1$  and  $\ell_2$ . In each case the bisectors are either hyperbolic paraboloids (HP), pairs of planes (2P), or single planes (P). The superscript <sup>s</sup> indicates singular trisectors. \*The number of connected components for cells  $V_{1,2}$  and  $V_{2,3}$  depends on whether the third skew line intersects the plane containing the parallel lines in between them or not.

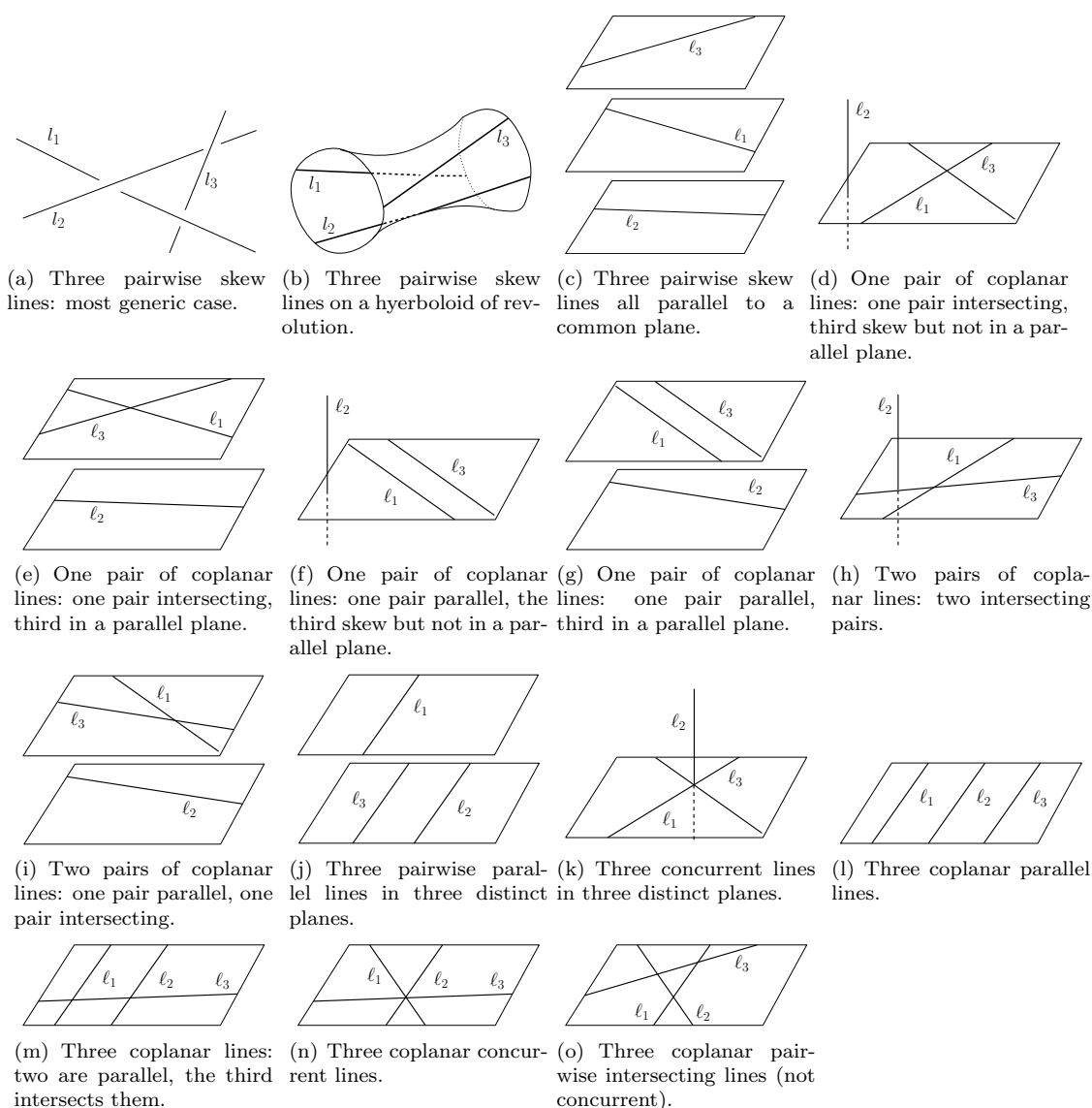


Figure 2: Classification of the degenerate cases.

- by space subdivision. *CGTA*, 21(3):87–120, 2002.
- [8] H. Everett, D. Lazard, S. Lazard, and M. S. E. Din. The Voronoi diagram of three lines in  $\mathbb{R}^3$ . In *SoCG'07*, pages 255–264, S. Korea, 2007.
- [9] M. . Karavelas. A robust and efficient implementation for the segment voronoi diagram. In *Proc. Internat. Symp. on Voronoi diagrams in Science and Engineering*, pages 51–62, 2004.
- [10] M. I. Karavelas. A robust and efficient implementation for the segment Voronoi diagram. In *International Symposium on Voronoi Diagrams in Science and Engineering*, pages 51–62, 2004.
- [11] V. Koltun and M. Sharir. Three dimensional euclidean Voronoi diagrams of lines with a fixed number of orientations. *SIAM Journal on Computing*, 32(3):616–642, 2003.
- [12] V. J. Milenkovic. Robust construction of the Voronoi diagram of a polyhedron. In *CCCG'93*, pages 473–478, 1993.
- [13] B. Mourrain, J.-P. T ecourt, and M. Teillaud. On the computation of an arrangement of quadrics in 3D. *CGTA*, 30(2):145–164, 2005.
- [14] E. Sch omer and N. Wolpert. An exact and efficient approach for computing a cell in an arrangement of quadrics. *CGTA*, 33(1-2):65–97, 2006.
- [15] M. Sharir. Almost tight upper bounds for lower envelopes in higher dimensions. *DCG*, 12:327–345, 1994.